Laser-controlled switching of molecular arrays in an dissipative environment

Gereon Floß, Tillmann Klamroth, and Peter Saalfrank
Theoretische Chemie, Institut für Chemie, Universität Potsdam, Karl-Liebknecht-Straße 24-25, D-14476 Potsdam-Golm
(Received 20 September 2010; revised manuscript received 14 January 2011; published 21 March 2011)

The optical switching of molecular ensembles in a dissipative environment is a subject of various fields of chemical physics and physical chemistry. Here we try to switch arrays of molecules from a stable collective ground state to a state in which all molecules have been transferred to another stable higher-energy configuration. In our model switching proceeds through electronically excited intermediates which are coherently coupled to each other through dipolar interactions, and which decay incoherently within a finite lifetime by coupling to a dissipative environment. The model is quite general, but parameters are chosen to roughly resemble the all-trans → all-cis isomerization of an array of azobenzene molecules on a surface. Using analytical and optimal control pulses and the concept of "laser distillation," we demonstrate that for various aggregates (dimers up to hexamers), controlled and complete switching should be possible.

DOI: 10.1103/PhysRevB.83.104301 PACS number(s): 82.20.Rp, 31.70.Hq, 33.80.−b

I. INTRODUCTION

In many situations encountered in atomic physics, condensed phase physics, molecular electronics, quantum computing, and biology, the problem arises that an individual quantum system (the "monomer," e.g., a spin, an atom, an adsorbate, or a chromophore) is being switched by an external perturbation from one stable state to another (meta)stable state, while at the same time being coupled to an array of other monomers and a dissipative environment.

Specific examples are qubits in traps, for example, exchange-coupled spins in external magnetic fields[1] or cold polar molecules in electric fields,[2,3] spectroscopy and excitonic energy transfer in molecular dye aggregates,[4] light-harvesting in photosynthetic systems,[5] and the light-induced conformational switching of functionalized molecular aggregates or self-assembled monolayers on solid substrates.[7]

Concerning the latter example, it has been shown experimentally that the light-induced ensemble switching of self-assembled monolayers (SAMs) of azobenzene-functionalized alkanethiols on gold surfaces from an all-trans to an all-cis form, is hampered by coherent exciton coupling which leads to ultrafast quenching of the initially excited electronic states.[7] In general, also incoherent processes (e.g., electronic coupling to an underlying metal surface) can cause fast quenching of excited intermediates. Finally, in densely packed molecular aggregates and SAMs steric hindrance can suppress switching.[8] To improve switching performance, it appears therefore necessary to (i) decouple the switching units from the surface, and (ii) to decouple the monomers from each other. Both can be achieved by using bulky linker groups. The first type of decoupling reduces incoherent (vertical) quenching, the second one coherent (lateral) energy transfer between the molecules. (iii) Finally, also the exciting light must be optimal to achieve large cross sections.

In this paper we address, in particular, the latter point by taking care of incoherent and coherent quenching mechanisms simultaneously. We study limitations to and possibilities for the collective photoswitching of molecular N aggregates from a stable initial state, $|t_1 t_2, \ldots, t_N\rangle$, to a final stable (or metastable) state, $|c_1 c_2, \ldots, c_N\rangle$. The notions "$t$" and "$c$" refer to "trans" and "cis" configurations of the monomers. However, the models to be developed below are more general. Further, m_α denotes a monomer α in level m, with $m = t$ or c. (The "states" or conformations of a monomer are called "levels" in the following; the notion "states" will be reserved for N-particle states.) The switching from levels t to c proceeds through electronically excited levels, e, which are populated by laser pulses. The excited states are coherently dipole-coupled to each other, and they decay incoherently with a certain lifetime, τ. The laser-driven dynamics is treated within an open-system density matrix framework in the basis of p^N direct-product states $|n_1 m_2, \ldots, k_N\rangle$, where p is the number of levels per monomer. Two models, one with $p = 3$ (t, c, and one e level per monomer), and another one with $p = 4$ (two e levels), are considered. We suggest several strategies of how to construct optimal pulses and pulse sequences for collective switching. In particular, a laser distillation scheme appears to be promising.

The paper is organized as follows. In the next section, the different models will be described, along with the equations of motion to treat the laser-driven dissipative aggregate dynamics. Section III describes the response of various N aggregates to ultrashort laser pulses, sequences of laser pulses, and continuous-wave-like laser fields. The final Sec. IV concludes and summarizes this work.

II. MODEL AND METHODS

A. Equations of motion

In the following, we wish to solve a Liouville–von-Neumann equation for the time evolution of the laser-driven, open-system density operator. Using a Markovian Lindblad form for dissipation, the equations of motion in the basis of M eigenstates $\{|n\rangle\}$ of the uncoupled, dissipation- and field-free system Hamiltonian are given by[9]

$$\frac{d\rho_{nn}}{dt} = -\frac{i}{\hbar}\sum_{i=1}^{M}(V_{ni}\rho_{in} - \rho_{ni}V_{in}) + \sum_{i=1}^{M}(\Gamma_{i\to n}\rho_{ii} - \Gamma_{n\to i}\rho_{nn}), \quad (1)$$

for the diagonal elements of the density matrix (state populations), and for the off-diagonal elements (coherences)

$$\frac{d\rho_{mn}}{dt} = -i\omega_{mn}\rho_{mn} - \frac{i}{\hbar}\sum_{i=1}^{M}(V_{mi}\rho_{in} - \rho_{mi}V_{in}) - \frac{1}{2}\sum_{k=1}^{M}(\Gamma_{m\to k} + \Gamma_{n\to k})\rho_{mn}. \quad (2)$$

In this work pure dephasing is neglected. The dissipative transition rates $\Gamma_{m\to n}$ account for incoherent effects, namely the short lifetime of excited states due to their coupling to not explicitly included degrees of freedom, including surface modes.

Further,

$$V_{mn}(t) = V_{mn}^{\text{stat}} - \mu_{mn}E(t), \quad (3)$$

are coherent, interstate coupling elements. The second term on the right-hand side (r.h.s.) accounts for the time-dependent field-aggregate coupling, treated here in semiclassical dipole approximation. We assume that the transition dipole with elements μ_{mn} is oriented parallel to a field vector with amplitude $E(t)$. The diagonal dipole matrix elements μ_{nn} are set to zero, which corresponds to neglecting Stark shifts of level $|n\rangle$. Test calculations applying permanent molecular dipoles characteristic for azobenzene and fields used in this work show that this is indeed an excellent approximation.

The static coupling terms V_{mn}^{stat} in Eq. (3) couple excited states. Specifically, they stand for couplings leading to exciton transfer between different monomers, or, in the case of the four-level models, for couplings between different excited states of a monomer. Details will be given below.

Finally, $\omega_{mn} = (E_m - E_n)/\hbar$ is the Bohr frequency between states $|m\rangle$ and $|n\rangle$ with energies E_m and E_n, respectively.

B. *N* monomers with three levels each

In a first model we consider N monomers, each with three levels t, c, and e. This is a very coarse-grained description of switching, where we assume that the multidimensional, double-well ground state potential energy surface can be represented by two levels t and c, respectively, and involved excited state potential energy surface(s) can be mapped onto a single level, e. For N noninteracting monomers, with uncoupled monomer levels and without dissipation and field, the system eigenstates are given as direct product states

$$|n\rangle = |k_1 l_2, \ldots, m_N\rangle, \quad (4)$$

with k, l, and m taking values t, c, and e, respectively. The corresponding state energies are

$$E_n = E_k + E_l + \cdots + E_m. \quad (5)$$

There are 3^N direct product states. For example, for the dimer $N = 2$ we have the nine states $|t_1t_2\rangle$, $|t_1c_2\rangle$, $|t_1e_2\rangle$, $|c_1t_2\rangle$, $|c_1c_2\rangle$, $|c_1e_2\rangle$, $|e_1t_2\rangle$, $|e_1c_2\rangle$, and $|e_1e_2\rangle$. The corresponding state energies are $2E_t$, $E_t + E_c$, $E_t + E_e$, and so forth. In rough agreement with experimental and quantum chemical data for isolated azobenzene, we set $E_t = 0$, $E_c = 0.6$ eV and $E_e = 4.0$ eV in the following.[10–12]

Each monomer can radiatively be excited/deexcited from/to the electronic ground state levels t and c, to/from the excited state e. The corresponding transition dipole moments are taken as $\mu_{te} = 2.894$ and $\mu_{ce} = 0.826$ a.u. from Ref. 12. In our model, for an N aggregate only one monomer can be radiatively excited at a time. For instance, for a dimer one has $\mu_{tt,ee} = \langle t_1(1)t_2(2)|\hat{\mu}(1) + \hat{\mu}(2)|e_1(1)e_2(2)\rangle = \langle t_1(1)|\hat{\mu}(1)|e_1(1)\rangle\langle t_2(2)|e_2(2)\rangle + \langle t_2(2)|\hat{\mu}(2)|e_2(2)\rangle\langle t_2(2)|e_2(2)\rangle = 0$, and simultaneous $|t\rangle \to |e\rangle$ excitation of both monomers is impossible. Hence, in the case of a dimer, for example, state $|t_1t_2\rangle$ is connected to state $|e_1t_2\rangle$ through μ_{te}. The doubly excited state $|e_1e_2\rangle$ can only be reached by two single excitations (e.g., through the sequence $|t_1t_2\rangle \overset{\mu_{te}}{\leftrightarrow} |e_1t_2\rangle \overset{\mu_{te}}{\leftrightarrow} |e_1e_2\rangle$).

Once in single- or multiply excited states, these cannot only be deexcited by optical means, but also incoherently, through dissipation. For a monomer, we assume for simplicity that the electronically unexcited levels $|t\rangle$ and $|c\rangle$ can both be reached within the same lifetime τ (i.e., $\Gamma_{e\to t} = \Gamma_{e\to c} = \Gamma = \tau^{-1}$). In what follows, we choose $\tau = 1$ ps. In the case of an N aggregate, we assume that only one incoherent deexcitation process occurs at a time, at the same monomer. Hence, in the case of a dimer, exemplarily the following relaxations are possible: $|e_1t_2\rangle \overset{\Gamma_{e\to t}}{\to} |t_1t_2\rangle$, $|e_1t_2\rangle \overset{\Gamma_{e\to c}}{\to} |c_1t_2\rangle$, $|c_1e_2\rangle \overset{\Gamma_{e\to c}}{\to} |c_1c_2\rangle$, $|e_1e_2\rangle \overset{\Gamma_{e\to c}}{\to} |c_1e_2\rangle \overset{\Gamma_{e\to t}}{\to} |c_1t_2\rangle$, and so forth. Dissipation is assumed to not couple different monomers.

However, in N aggregates excited levels are coherently coupled to other monomers through dipolar coupling terms, (i.e., $V_{mn}^{\text{stat}} = V_{mn}^{\text{dip}}$). For instance, in the case of a dimer we assume that state $|e_1t_2\rangle$ is coupled to state $|t_1e_2\rangle$, and state $|e_1c_2\rangle$ to state $|c_1e_2\rangle$. Both situations correspond to coherent exciton transfer, and are described in the following by a universal coupling matrix element V_1, where the index "1" refers to first-neighbor coupling. In a point-dipole approximation assuming two parallel transition dipole moments of strength μ_0 (= μ_{te} or μ_{ce}, respectively), at nearest-neighbor distance d_0, the coupling strength is $V_1 = \mu_0^2/d^3$.[6] Below in all cases we choose $V_1 = 3.927 \times 10^{-3}$ a.u. (∼0.1 eV). This value is of the order of magnitude estimated from typical transition dipole moments (see below) and nearest-neighbor distances d_0 (∼10 a.u.) for azobenzene SAMs on Au(111) as studied in Ref. 7. The chosen V_1 gives, according to the Rabi formula for a coupled, degenerate two-level system, a transfer time $t = \pi\hbar/(2V_1) = 10$ fs, which is also consistent with time-resolved measurements for the same system.[7]

For N-mers, we parametrize the exciton transfer matrix elements between two monomers α and β due to a dipole coupling mechanism as

$$V_{mn}^{\text{dip}} \to V_{\alpha\beta}^{\text{dip}} = \frac{V_1}{(d_{\alpha\beta}/d_0)^3}. \quad (6)$$

Here, $(d_{\alpha\beta}/d_0)$ is the ratio of the distance between the two exciton-exchanging monomers α and β, to the nearest-neighbor "reference" distance between two monomers, d_0. Assuming that the latter is the same for all aggregates, that means that, for example, in a linear trimer, the coupling between states $|e_1t_2t_3\rangle$ and $|t_1e_2t_3\rangle$ of V_1 reduces to $V_1/8$ if $|e_1t_2t_3\rangle$ couples to $|t_1t_2e_3\rangle$. We assume that all exciton transfer events are energy conserving.

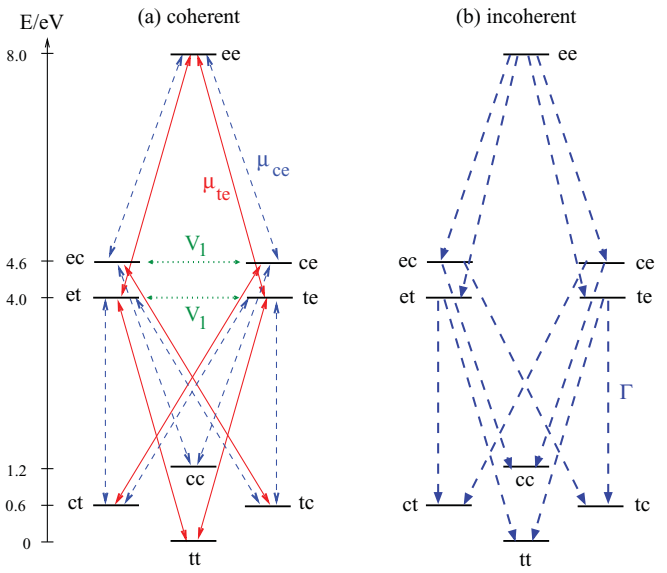

FIG. 1. (Color online) Term diagram for a dimer consisting of three-level monomers. (a) Coherent couplings. Nonhorizontal lines indicate field-system couplings $-\mu_{te}E(t)$ (red) and $-\mu_{ce}E(t)$ (blue), respectively, and horizontal green lines the dipole couplings V_1. The parameter choices are $\mu_{te} = 2.894$ a.u., $\mu_{ce} = 0.826$ a.u., and $V_1 = 3.927 \times 10^{-3}$ a.u. (b) Incoherent relaxation processes. For all transitions the same $\Gamma = (1\ \text{ps})^{-1}$ was used. For all states, a self-evident shorthand notation was used, e.g., te instead of $|t_1 e_2\rangle$.

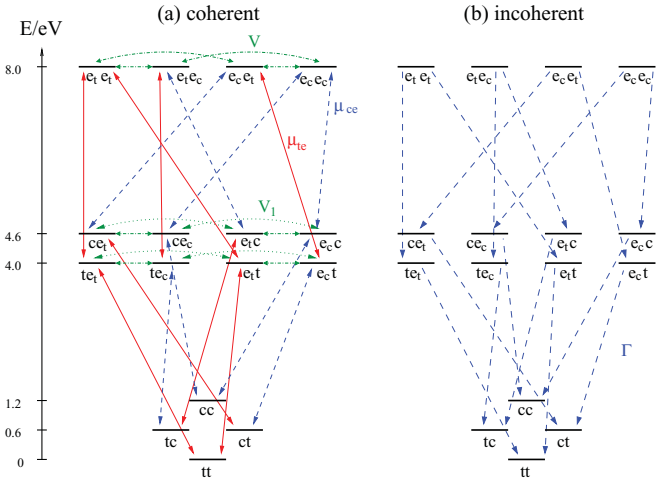

FIG. 2. (Color online) Term diagram for a dimer consisting of four-level monomers. (a) Coherent couplings. Nonhorizontal lines indicate field-system couplings $-\mu_{te}E(t)$ (red) and $-\mu_{ce}E(t)$ (blue), respectively. Horizontal green lines denote dipolar couplings V_1 between different monomers (dotted), and the $e_c \leftrightarrow e_t$ couplings V within a monomer (solid). The parameter choices are as before, and $V = 7.599 \times 10^{-5}$ a.u. (b) Incoherent relaxation processes. For all transitions, the same $\Gamma = (1\ \text{ps})^{-1}$ was used. Again, a shorthand notation was used for the states.

Finally, we assume that the c levels are stable and cannot relax directly to t levels. Thus we neglect, for example, the thermal isomerization from $|c_1 t_2\rangle$ to $|t_1 t_2\rangle$.

For clarity, we summarize the model in Fig. 1 for the dimer case. Figure 1(a) shows coherent processes, Fig. 1(b) incoherent (relaxation) transitions.

Below we will consider dimers, linear trimers, tetramers, pentamers and hexamers, trigonal trimers, and quadratic tetramers.

C. N monomers with four levels each

The results obtained with three-level monomers suggest that the $t \to c$ transition, once the excited level e was reached, can be almost instantaneous. If the model is to represent azobenzene switching, however, one needs to consider the time evolution in the excited state from trans-like toward cis-like geometries. Thus there is a finite reaction time, in the order of a few hundred femtoseconds for azobenzene according to theory[8] and time-resolved measurements.[13]

Within our coarse-grained model which neglects wave packet motion on potential energy surfaces, we account for this time delay by using a four-level monomer comprising levels t, c, e_t, and e_c. The electronically excited levels e_t and e_c can be seen as belonging to the same excited state potential energy surface, but different geometries. For simplicity, we assume that they have the same energy, $E_{e_t} = E_{e_c} = E_e = 4.0$ eV. The finite reaction time is modeled by a coherent coupling V between e_t and e_c on the same monomer. With the choice $V = 7.599 \times 10^{-5}$ a.u., we get a Rabi transfer time of 500 fs, in accordance with Refs. 13 and 14. In the four-level model, a dipole moment μ_{te} allows for radiative coupling of levels t and e_t, and transition dipole moment μ_{ce} couples c and e_c. Dissipation induces transitions from e_t to t, and from e_c to c, with a common rate Γ, again chosen as $\Gamma = (1\ \text{ps})^{-1}$. Otherwise the four-level model is analogous to the three-level model. The corresponding coherent and incoherent transitions are indicated in Fig. 2. For the four-level model, only the dimer was considered for simplicity.

D. Laser pulse sequences

The goal is to optimize the yield of the collectively switched $|c_1 c_2, \ldots, c_N\rangle$ target state, starting from the most stable ground state configuration, $|t_1 t_2, \ldots, t_N\rangle$:

$$|t_1 t_2, \ldots, t_N\rangle \to |c_1 c_2, \ldots, c_N\rangle. \tag{7}$$

This shall be achieved by a sequence of L $\sin^2$-shaped laser pulses

$$E(t) = \sum_{k=1}^{L} E_{0k} \cdot \sin^2\left(\frac{\pi(t - t_{0k})}{\sigma_k}\right) \cdot \cos[\omega_k(t - t_{0k})]. \tag{8}$$

In Eq. (8), pulse k starts at $t = t_{0k}$ and has duration σ_k; outside the interval $[t_{0k}, t_{0k} + \sigma_k]$ the contribution of the kth term to the field is set to be zero. Further, ω_k is the respective laser carrier frequency, and E_{0k} the pulse amplitude. The latter can be chosen to fulfill the π-pulse condition for level inversion in a dissipation-free two-state system under the rotating wave approximation. In this case one has, for $\sin^2$ pulses enforcing a transition $|m\rangle \to |n\rangle$[9]

$$E_{0k}^{\pi} = \frac{2\pi\hbar}{\sigma_k |\mu_{mn}|}. \tag{9}$$

Since our systems consist of more than two states, it can be useful to reoptimize the parameters in Eq. (8) "by hand," or, more elegantly, one can use various forms of optimal control theory for dissipative dynamics[9,15,16] instead.

III. RESULTS

A. Single pump-dump sequences

1. Analytic pulses

Let us first consider strategies based on the application of short pulses to enforce the reaction (7) by a single "pump-dump" sequence. We start with the three-level dimer (cf., Fig. 1), applying a series of π pulses. From Fig. 1 it is evident that by lateral coupling elements V_1 previously degenerate states $|e_1t_2\rangle$ and $|t_1e_2\rangle$ will Davydov split into two states

$$|\psi_{et}^{+}\rangle = \frac{1}{\sqrt{2}}(|e_1t_2\rangle + |t_1e_2\rangle), \tag{10}$$

$$|\psi_{et}^{-}\rangle = \frac{1}{\sqrt{2}}(|e_1t_2\rangle - |t_1e_2\rangle), \tag{11}$$

with energies $E_{et}^{+} = E_e + E_t - V_1 \approx 4.1$ eV and $E_{et}^{-} = E_e + E_t + V_1 \approx 3.9$ eV, respectively. Similarly, the pair $|e_1c_2\rangle$ and $|c_1e_2\rangle$ splits into states $|\psi_{ec}^{+}\rangle$ and $|\psi_{ec}^{-}\rangle$, with energies $E_{ec}^{+} = E_e + E_c - V_1 \approx 4.7$ eV and $E_{ec}^{-} = E_e + E_c + V_1 \approx 4.5$ eV, respectively. We therefore suggest a sequence of four π pulses,

$$|t_1t_2\rangle \overset{\omega_1,\sqrt{2}\mu_{te}}{\rightarrow} |\psi_{et}^{+}\rangle \overset{\omega_2,\sqrt{2}\mu_{te}}{\rightarrow} |e_1e_2\rangle \overset{\omega_3,\sqrt{2}\mu_{ce}}{\rightarrow} |\psi_{ec}^{+}\rangle \overset{\omega_4,\sqrt{2}\mu_{ce}}{\rightarrow} |c_1c_2\rangle. \tag{12}$$

The isomerization pathway consists of a single "pump" and a subsequent "dump" sequence, where $\hbar\omega_1$ and $\hbar\omega_2$ enforce pumping, and $\hbar\omega_3$ and $\hbar\omega_4$ the dumping. The + (gerade) states serve as intermediate states. The transition energies are $\hbar\omega_1 = E_{et}^{+} - E_t \approx 4.1$ eV, $\hbar\omega_2 = 2E_e - E_{et}^{+} \approx 3.9$ eV, $\hbar\omega_3 = 2E_e - E_{ec}^{+} \approx 3.3$ eV, and $\hbar\omega_4 = E_{ec}^{+} - 2E_c \approx 3.5$ eV, respectively. The transition dipole moments are analytically given as $\sqrt{2}\mu_{te}$ and $\sqrt{2}\mu_{ce}$. Transitions to the − (ungerade) states are symmetry forbidden. In passing we note that the $|t_1t_2\rangle \rightarrow |\psi_{et}^{+}\rangle$ transition, for example, is hypsochromically (blue) shifted relative to a $|t\rangle \rightarrow |e\rangle$ monomer transition.[6]

This stepwise strategy can be quite successful, as demonstrated in Fig. 3. There, four nonoverlapping $\sin^2$ pulses with duration $\sigma_k = 2000$ a.u. (≈50 fs) each were applied, giving a final state population of 0.850 for the dimer. The small loss of about 0.15 is due to the finite width of the laser pulses due to more than two coupled states being involved, and due to dissipation. The applied, maximal π-pulse intensities are moderately high with 2.07×10^{10} W/cm^2 for the pump, and 2.54×10^{11} W/cm^2 for the dump pulses, respectively.

The realization of Eq. (7) with analytic pulses of the form (8) becomes more cumbersome as the number of units, N, increases. For an N-mer, there are states with one up to N excitons which can be used as intermediates. In the uncoupled case, there are groups of $\frac{N!}{m!(N-m)!}$ degenerate m-exciton states, for each possible combination of the remaining $(N-m)$ levels of the t and c type. For example, for the trimer $N = 3$ we have three single-exciton states $|e_1b_2b_3'\rangle$, $|b_1e_2b_3'\rangle$, $|b_1b_2'e_3\rangle$ for each b, $b' = t$ or c with energy $E_e + E_b + E_{b'}$. There

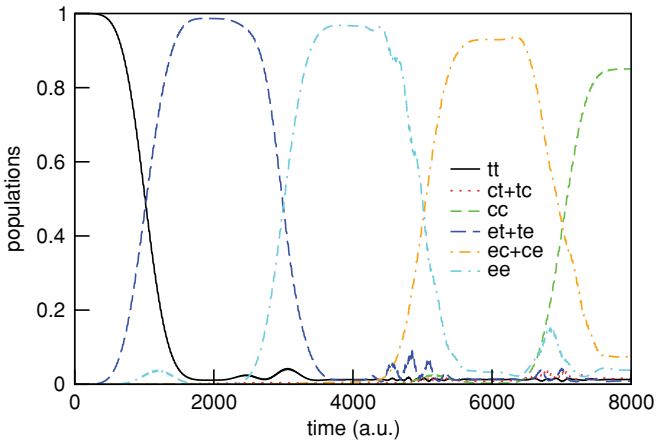

FIG. 3. (Color online) Dimer consisting of three-level systems: Populations of initial, final, and various intermediate states, for a four π-pulse strategy (7), as a function of time. A pulse sequence (8) was used, with $L = 4$, and $E_{01} = E_{02} = 7.677 \times 10^{-4}$ a.u., $E_{03} = E_{04} = 2.689 \times 10^{-3}$ a.u.; $t_{01} = 0$, $t_{02} = 2000$ a.u., $t_{03} = 4000$ a.u., $t_{04} = 6000$ a.u.; $\sigma_1 = \sigma_2 = \sigma_3 = \sigma_4 = 2000$ a.u.; $\omega_1 = 0.150\,93$ a.u., $\omega_2 = 0.143\,07$ a.u., $\omega_3 = 0.121\,02$ a.u., and $\omega_4 = 0.128\,87$ a.u.

are also three bi-exciton states $|e_1e_2b_3\rangle$, $|e_1b_2e_3\rangle$, $|b_1e_2e_3\rangle$ with energy $2E_e + E_b$. Each degenerate group broadens into a band if exciton coupling is present. For linear chains with nearest-neighbor couplings only, the band width is $4V_1$ in the limit $N \rightarrow \infty$. There are allowed and forbidden transitions to and from these possible intermediate states. All of the intermediate states have finite lifetimes. In general, the determination of optimal sequential pathways and corresponding resonance frequencies and other π-pulse parameters becomes impractical. The strategy becomes also unselective because the idealizations valid for π pulses do not hold anymore.

We avoid the problem by using very short pump and dump π pulses tuned to the energy of uncoupled excited states. The pulses are energetically broad and therefore able to excite several intermediate states simultaneously. We illustrate this for the four-level dimer (cf., Fig. 2). In Fig. 4, we use a sequence of two pulses, both of duration 400 a.u. (≈10 fs) to enforce the reaction

$$|t_1t_2\rangle \overset{\omega_1,\mu_{te}}{\rightarrow} \text{states with } e_t \overset{V}{\rightarrow} \text{states with } e_c \overset{\omega_2,\mu_{ce}}{\rightarrow} |c_1c_2\rangle. \tag{13}$$

The excitation energy of the pump pulse was chosen as $\hbar\omega_1 = E_e = 4$ eV, and the field amplitude according to Eq. (9) with $\mu_{mn} = \mu_{te_t} = \mu_{te}$. The pump-pulse populates intermediate single-exciton states, namely linear combinations of $|t_1e_{t,2}\rangle$ and $|e_{t,1}t_2\rangle$, and from there the double excitations, $|e_{t,1}e_{t,2}\rangle$. These intermediate states contain e_t levels, which then couple through the V matrix elements to states with e_c levels such as $|e_{c,1}e_{c,2}\rangle$. The $e_t \rightarrow e_c$ transport takes about 500 fs, or roughly 20 000 a.u.. When applying after about that time a dump laser pulse with energy $\hbar\omega_2 = E_e - E_c = 3.4$ eV and field amplitude $E_0 = 2\pi\hbar/(\mu_{ce}\sigma_2)$, the system can be deexcited toward the $|t_1t_2\rangle$ target state. Although both the pump and the dump pulses appear to be quite efficient, the final yield after $t = 25\,000$ a.u. is only around 35% for a pump-dump delay time of 18 700 a.u. because during the "isomerization time" population is lost to other states, mostly by incoherent decay.

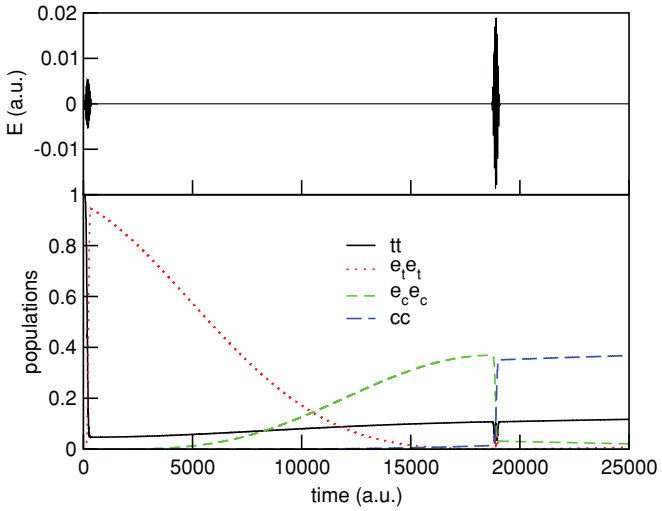

FIG. 4. (Color online) Two-pulse pump and dump strategy for the isomerization of a dimer of four-level monomers. The upper panel shows the pulses, the lower one the populations of the all-trans, the all-cis, and the doubly excited states $|e_{t,1}e_{t,2}\rangle$ and $|e_{c,1}e_{c,2}\rangle$. Pulses have duration $\sigma_1 = \sigma_2 = 400$ a.u., delayed by 18 700 a.u. (ca. 450 fs), i.e., $t_{01} = 0$ and $t_{02} = 18\,700$ a.u. Frequencies and field amplitudes are $\omega_1 = 0.146\,99$ a.u., $E_{01} = 5.43 \times 10^{-3}$ a.u., $\omega_2 = 0.124\,95$ a.u., and $E_{02} = 1.90 \times 10^{-3}$ a.u.

The target yield as a function of delay time between the pump and dump pulse is shown in Fig. 5, for two different pulse lengths $\sigma_1 = \sigma_2$ of 400 and 1000 a.u., respectively. We observe that (i) the target yield has a maximum close to the Rabi transfer time $t = \pi\hbar/(2V)$ of 500 fs, and (ii) that shorter pulses give a better yield. With our pump-dump strategy we achieve target yields in the order of 22% with the longer pulses, which, however, have lower intensities and are therefore experimentally more feasible.

2. *Pulses from optimal control theory*

Before addressing larger aggregates and other control strategies to optimize all-cis yields, let us first consider the short-pulse pump-dump strategy in connection with optimal control theory (OCT) as an alternative to analytical pulses. We use the same, global OCT algorithm as in Refs. 9,16, where the expectation value of a target operator $\hat{O}$ (i.e., $\langle\hat{O}\rangle = \mathrm{Tr}\{\hat{\rho}\,\hat{O}\}$), is to be maximized at the end of the laser pulse, t_f. Additional constraints are that (i) the dissipative equations of motion (1) and (2) are obeyed, and (ii) a penalty function is introduced to restrict the maximal laser intensity.[17] This results in an iterative process to obtain the optimal field, $E(t)$, including forward propagations starting from the initial density operator $\hat{\rho}_0$, and backward propagations starting from the final target operator $\hat{O}$ at time t_f.

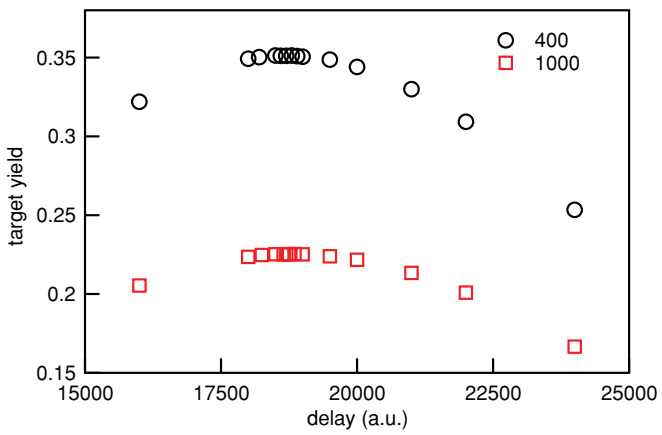

FIG. 5. (Color online) Yield of the all-cis target state using a pump-dump scheme for the four-level dimer as a function of the delay time between the pulses. Circles denote pulses with a length of 400 a.u. and squares denote pulses with a length of 1000 a.u.

As there is no direct coupling between $|t\rangle$ and $|c\rangle$ we were unsuccessful in computing a field that switches the system by directly defining $\hat{\rho}_0 = |t_1t_2,\ldots,t_N\rangle\langle t_1t_2,\ldots,t_N|$ and $\hat{O} = |c_1c_2,\ldots,c_N\rangle\langle c_1c_2,\ldots,c_N|$. Rather, two separate control fields were constructed first, one for exciting the system within a pump time, $t_{f,\mathrm{pump}}$, and one for deexciting it within a dump time, $t_{f,\mathrm{dump}}$. In the case of three-level monomers, the pump field is computed with the choice $\hat{\rho}_0 = |t_1t_2,\ldots,t_N\rangle\langle t_1t_2,\ldots,t_N|$, starting at $t = 0$, and $\hat{O} = |e_1e_2,\ldots,e_N\rangle\langle e_1e_2,\ldots,e_N|$ to be reached after $t_{f,\mathrm{pump}}$. The dump field is computed with the choice $\rho_0 = |e_1e_2,\ldots,e_N\rangle\langle e_1e_2,\ldots,e_N|$ starting at $t = t_{f,\mathrm{pump}}$, and $\hat{O} = |c_1c_2,\ldots,c_N\rangle\langle c_1c_2,\ldots,c_N|$ the target to be reached after $t = t_{f,\mathrm{pump}} + t_{f,\mathrm{dump}}$. The final field is obtained by combining the two pieces, and globally reoptimizing using the OCT algorithm with the choice $\hat{\rho}_0 = |t_1t_2,\ldots,t_N\rangle\langle t_1t_2,\ldots,t_N|$ at $t = 0$, and $\hat{O} = |c_1c_2,\ldots,c_N\rangle\langle c_1c_2,\ldots,c_N|$ to be reached at $t = t_f = t_{f,\mathrm{pump}} + t_{f,\mathrm{dump}}$. In practice, we chose $t_{f,\mathrm{pump}} = t_{f,\mathrm{dump}} = 400$ a.u..

An OCT field was determined for the dimer, leading to a target yield of 0.891. The field and state populations are shown in Fig. 6. This yield is about what has been achieved

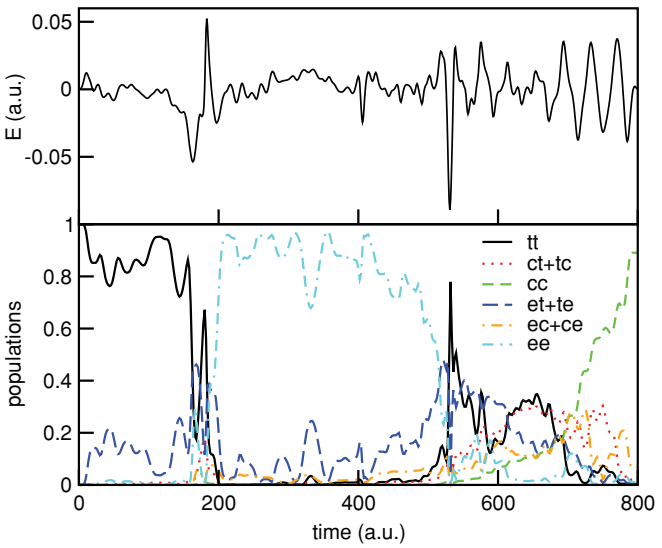

FIG. 6. (Color online) Optimal control strategy for the isomerization of a dimer consisting of three-level monomers. The upper panel shows the optimal laser field, the lower one the populations of the all-trans, the all-cis, and selected intermediate states. The total control time is $t_f = 800$ a.u., the pump and dump control times are 400 a.u. each (see text).

with a sequence of four analytical pulses in Fig. 3, however, within a much shorter time, and without the need to select transition frequencies in advance. The former advantage can be important for systems which are even more dissipative than those studied here, and the latter helps if the systems are too complex to guess simple excitation pathways beforehand. We note that the OCT pulse is rather broad in frequency space (not shown), that is, a simple assignment of clear transition frequencies was not possible. The efficiency of the OCT scheme as applied here decreases with increasing system size: For the hexamer, for example, the final target yield is 0.677. It is to be expected, however, that better performance can be achieved by choosing a different control time, or defining (other) intermediate targets. In general, the OCT scheme can be a versatile tool also for molecular ensembles.

B. Laser distillation

1. General setup

The problem of photoisomerization from one stable state to another via dissipative intermediates, is ideally suited for "laser distillation." Within this concept one repeats a pump-dump sequence many times, thus gradually increasing the yield of the target. Therefore, it is not necessary that a single pump-dump sequence gives very high yields already. If the intermediates can directly decay to the target by dissipation, as here, one may even abandon the optical dump step. Laser distillation has theoretically been suggested to be useful for isomerization of adsorbates at surfaces,[18] for laser purification of enantiomers,[19–22] and for subsurface absorption.[23] Experimentally, the scheme was used, with continuous wave lasers, in materials science.[24] Here we suggest to adopt it for optical switching of molecular arrays.

In practice, we use a series of pump pulses (no dump pulses) to excite the initial all-trans state, with field-free intervals between the pulses. During the field-free intervals a partial decay into the target all-cis state occurs. Possible pump pulses are OCT pulses, or analytic π pulses for the $t \rightarrow e$ transition. The results below are for π pulses. A pulsed laser distillation scenario can be characterized by the pulse duration and the repetition interval, both of which are external control parameters. As an additional, internal parameter the lateral dipole coupling $V_1/(d/d_0)^3$ is varied below. In what follows we use pulse durations between 400 a.u. (ca. 10 fs) and 5000 a.u. (ca. 125 fs). The repetition time is between 400 fs (16 500 a.u.) and 1 ps (41 300 a.u.). As lateral coupling constant V_1, values between 3.927×10^3 a.u. (0.1069 eV), and 3.927×10^{-6} a.u. (0.1069 meV) were applied. For the last value, the Rabi oscillation time is 40 000 a.u. (ca. 10 ps). For the dimer, a systematic variation of all parameters in the mentioned intervals was performed, and in all cases the pulse was repeated 12 times. For the linear and trigonal trimers and the linear and quadratic tetramer pulse durations of 400 and 5000 a.u. were considered, with a repetition time of 400 fs and 1 ps. The linear pentamer was propagated with 400 and 5000 a.u. pulses and a repetition time of 1 ps. The linear hexamer was propagated with 400 a.u. pulses and a repetition time of 1 ps. For these N-mers with $N \geqslant 3$, lateral couplings of 3.927×10^{-3} a.u. and 3.927×10^{-6} a.u. were tested.

2. N monomers with three levels each

In Fig. 7 we show, for various N-mers with three-level monomers, the population of selected states as a function of time, if the laser distillation scheme is applied. In all cases, 12 pulses of duration 400 a.u. and a repetition time of 1 ps were used. In the figure, the pump pulses are so short compared to the total propagation time that state populations seem to change abruptly during the application of the pulse. It is seen that in practically all cases (i) the initial state $|t_1 t_2, \ldots, t_N\rangle$ (denoted "t" for short in the figure) is depopulated after a few pulses, while (ii) at the same time the population in the target state $|c_1 c_2 \ldots, , c_N\rangle$ ("c") increases more or less continuously; mixed states, including those which carry excitons, serve as intermediate states whose population grows and then falls. Note that for the larger N-mers (e.g., the hexamer) the all-cis population occurs delayed. That is, the first pulse creates almost no target state population in this case.

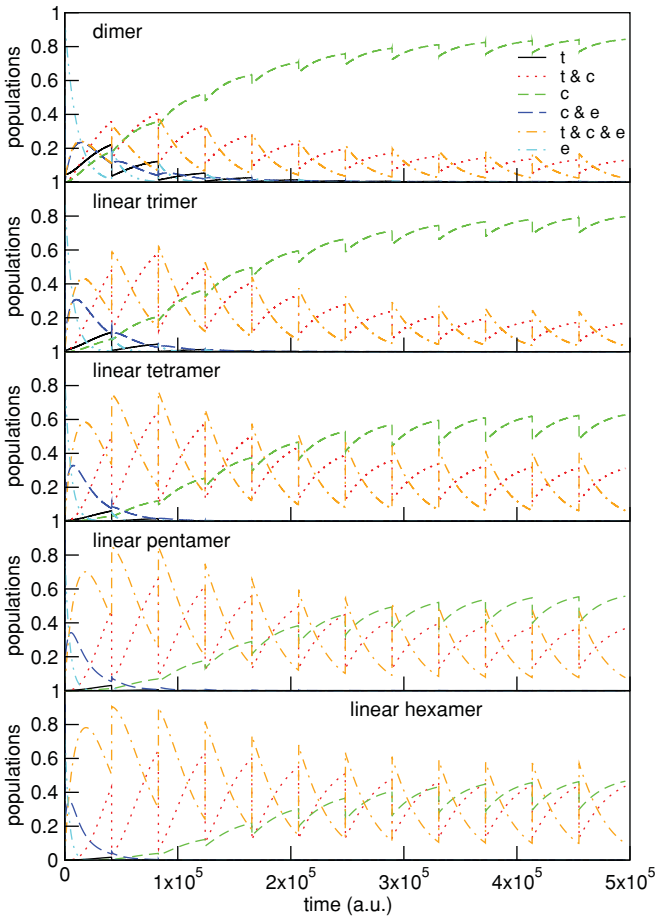

FIG. 7. (Color online) Performance of laser distillation. Shown are selected state populations of the dimer, linear trimer, linear tetramer, linear pentamer, and linear hexamer under the influence of laser distillation with pulse durations of 400 a.u. and a pulse repetition time of 1 ps. In all cases, three-level monomers were considered. The shorthand notation t stands for the all-trans initial state, c for the all-cis target state, and e for the N-exciton all-e state. The symbols t & c, c & e, and t & c & e denote the sum of all populations of mixed states with either two (t & c, e & c) or three (t & c & e) different components.

Closer inspection shows that the laser distillation works by taking two paths. The direct path is exciting the system from $|t_1t_2,\ldots,t_N\rangle$ to $|e_1e_2,\ldots,e_N\rangle$, transiently populating all mixed states with e and t contributions *en route*. From $|e_1e_2,\ldots,e_N\rangle$, the system then relaxes via mixed states into states $|t_1t_2,\ldots,t_N\rangle$ and $|c_1c_2,\ldots,c_N\rangle$, and states with both c and t contributions. In the case of the dimer a considerable amount reaches $|t_1t_2,\ldots,t_N\rangle$ and $|c_1c_2,\ldots,c_N\rangle$ already after the first pulse. In larger systems the number of combination states containing c and t increases and thus more population is trapped in those states. In fact, the "pure" states $|t_1t_2,\ldots,t_N\rangle$ and $|e_1e_2,\ldots,e_N\rangle$ play no role after the second pulse for $N \geqslant 3$. Here the second path comes into play: States representing ensembles of some molecules in trans and some molecules in cis configuration can still be excited such that some of the molecules in trans are now in an e level. Those relax with equal probability to trans and cis. After a few iterations, even the hexamer is switched to all-cis.

In Table I, we show the target yields obtained after 12 distillation steps, for certain N-mers and with the same repetition time of 1 ps as in Fig. 7. Different pulse lengths σ were examined. In many cases the final-time populations are above 0.8, indicative of an efficient switching process. We also note that the yield can be further optimized when applying longer distillation sequences. For now, the following observations can be made.

(i) While short pulses are generally more efficient in pumping the system from all-trans to all-cis, the laser distillation with pulse durations of 400 a.u. is less efficient than the laser distillation with pulse durations of 1000 a.u. Extremely short pulses do not only induce transitions from $|t_1t_2\rangle$ to $|e_1t_2\rangle/|t_1e_2\rangle$ and $|e_1e_2\rangle$, but due to the spectral broadening, also from the target state $|c_1c_2\rangle$ to $|c_1e_2\rangle/|e_1c_2\rangle$.

TABLE I. Target yields after twelve 1 ps steps during laser distillation of various N-mers, for three different pulse durations σ each.

N-mer	Pulse duration σ/a.u.	Target yield
Dimer	400	0.843
	1000	0.934
	5000	0.198
Linear trimer	400	0.797
	1000	0.795
	5000	0.0115
Trigonal trimer	400	0.632
	1000	0.701
	5000	$2.07 \cdot 10^{-3}$
Linear tetramer	400	0.627
	1000	0.833
	5000	$5.79 \cdot 10^{-3}$
Quadratic tetramer	400	0.554
	1000	0.748
	5000	$4.01 \cdot 10^{-4}$
Linear pentamer	400	0.557
	1000	0.788
	5000	0.0391
Linear hexamer	400	0.466
	1000	0.727
	5000	$3.69 \cdot 10^{-3}$

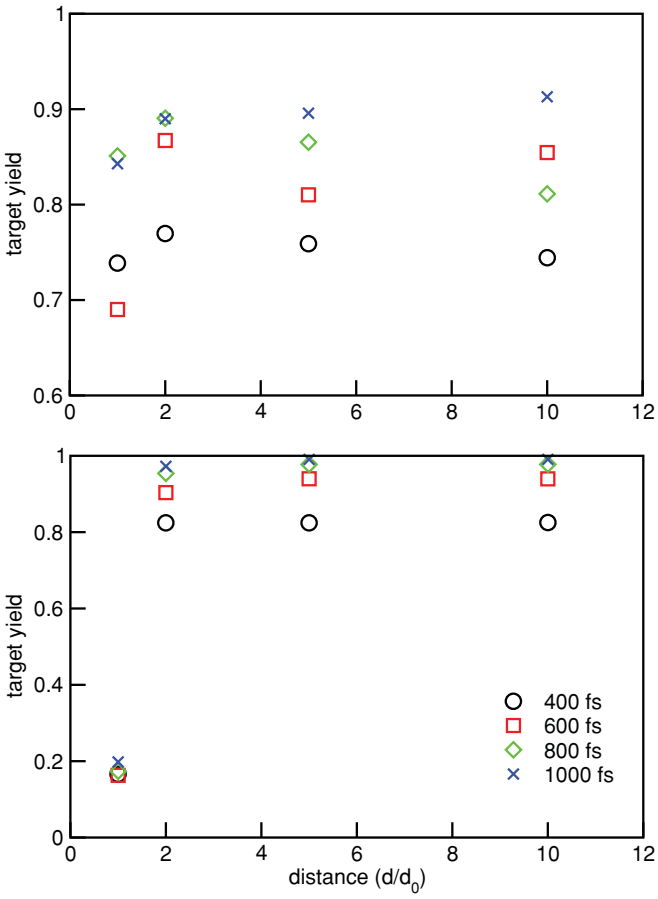

FIG. 8. (Color online) Target yield after a 12-pulse laser distillation sequence for the three-level dimer with different repetition times as a function of monomer-monomer distance given in units of a reference distance, d_0. The different types of symbols correspond to different repetition times ranging from 400 fs to 1ps. The pulse duration is 400 a.u. in the upper panel, and 5000 a.u. in the lower one.

(ii) The switching efficiency for larger aggregates depends more strongly on the pulse duration: For pulses with a duration of 400 and 1000 a.u. the efficiency varies only weakly with N, while it decreases considerably with system size for the pulses with a duration of 5000 a.u.

(ii) The more compact N-mers i.e., trigonal vs. linear trimer and quadratic vs. linear tetramer lead to slightly lower target yields after the end of the scheme. Note that in the compact N-mers the average distances are smaller and therefore exciton couplings larger.

The other external parameter of a laser distillation is the duration of the relaxation period. An internal parameter is the excitonic coupling strength $V_1/(d/d_0)^3$. In Fig. 8 we test both parameters simultaneously, by showing the target yield for the three-level dimer after twelve distillation steps for different repetition times, and as a function of decreasing coupling strength. On the abscissa we give the ratio d/d_0, i.e., the coupling strength is controlled here *via* the distance between the monomers.

From the figure, which is shown for two different pulse lengths of 400 (upper) and 5000 a.u. (lower), respectively, the following can be seen.

(i) The dependence of yield on repetition time for the long-pulse case is simple: With a longer gap between the pulses the yield is always increased because every single pulse becomes more efficient. This is also true for all pulse lengths considered (but most of them not shown), except for the case with $\sigma = 400$ a.u., where the trend is no longer clear.

(ii) The exciton coupling strength or, in other words, the monomer-monomer distance, is even more important. If the coupling is small (distance large), the switching of the entire ensemble is practically quantitative, in particular if the gap is large enough and the pulse width not too small (cf., Fig. 8, lower panel).

3. N monomers with four levels each

The laser distillation strategy is also useful for systems with four-level monomers. Here the same π pulses can be used and the mechanism remains analogous. The difference is the relaxation from the excited state to state $|c_1 c_2, \ldots, c_N\rangle$, which is not direct but delayed by about 500 fs. This is due to the fact that after excitation from a t level first an e_t level is reached, followed by transport of population to e_c, from where the system is finally dumped or relaxes to, the target c level. This is demonstrated in Fig. 9, where a dimer consisting of four-level monomers was stimulated again by a series of 12 pulses of width 400 a.u. each and with delay time 1 ps. It is seen that the first pulse, for example, first creates the doubly excited trans configuration, while the doubly excited cis configuration is delayed by about 20 000 a.u. (500 fs). Other than that, also in the case of four-level monomers, the laser distillation scheme works fine.

4. "Continuous-wave" laser excitation

As mentioned above, single pulses become inefficient for excitation and switching if they are too long because then the spectral width is too small to meet the resonance conditions.

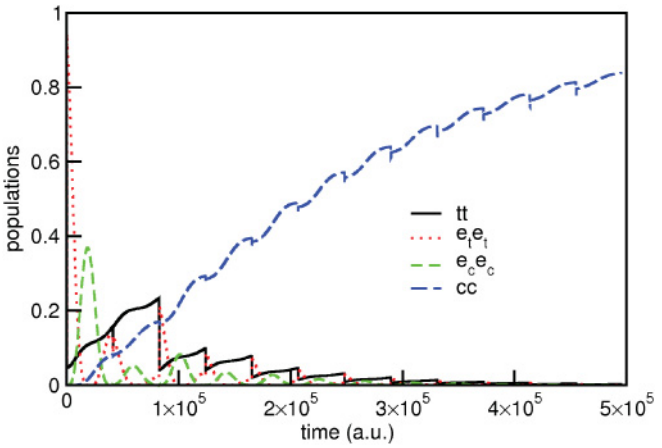

FIG. 9. (Color online) Performance of laser distillation for a dimer consisting of two four-level monomers. π pulses for $t \rightarrow e_t$ excitation of length 400 a.u. and with a pulse repetition time of 1 ps were used. Shown are the populations of the initial (all-trans, t), final (all-cis, c), and doubly excited (e_t and e_c) states.

Thus, the laser distillation scheme in its present form seems to be restricted to relatively short pulses, at least if there is nonvanishing exciton dipole coupling. A simple workaround which allows one to perform laser distillation in the continuous-wave limit is to use a superposition of continuous waves consisting of all possible excitation frequencies, ω_i. The laser field is thus chosen as

$$E(t) = \sum_{i=1}^{N} E_0 \cos(\omega_i t), \tag{14}$$

where $\hbar\omega_i$ are the possible excitation energies, starting from the all-trans state. These energies were obtained by diagonalizing the Hamiltonian of a subsystem containing all singly excited states. For example, in the case of a linear N-mer consisting of three-level monomers, this Hamiltonian is an $N \times N$ matrix with elements

$$H_{ij} = E_e \delta_{ij} + (1 - \delta_{ij}) V_{ij}^{\text{stat}}. \tag{15}$$

This way we calculate all possible transition energies from the all-trans state to the first exciton band, and also all transition energies between different exciton bands. The philosophy is thus very similar to Sec. III A 1, where the exact transition energies were used for excitation, albeit with laser pulses (cf., Fig. 3). Note also that the field (14), consisting of

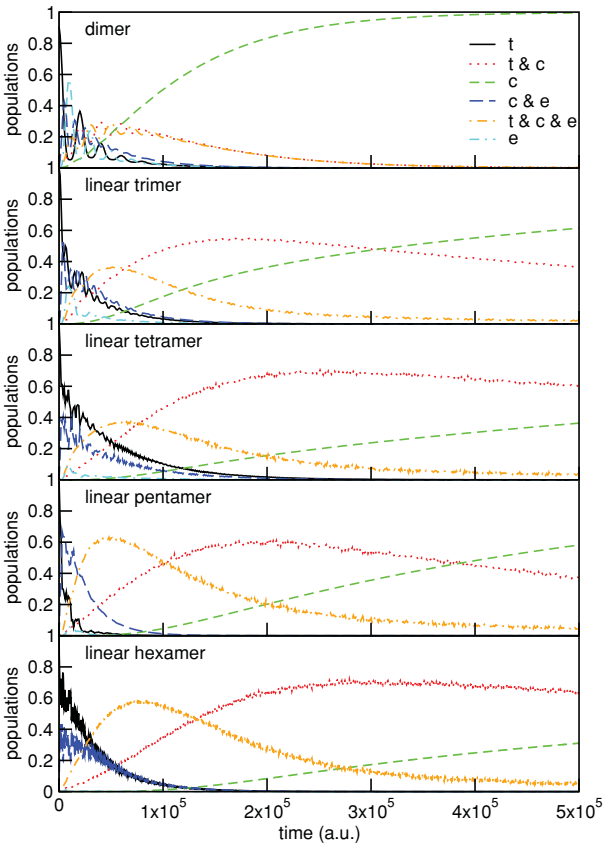

FIG. 10. (Color online) Performance of the "cw" distillation scheme for N-mers consisting of three-level monomers. Shown are the populations of the dimer, linear trimer, linear tetramer, linear pentamer, and linear hexamer as a function of time. Notation as in Fig. 9.

interfering partial waves, is not an ordinary continuous wave (cw) field.

For three-level monomers, the laser field (14) is able to excite any of the tested systems from dimer to hexamer in a given time. Figure 10 demonstrates this for the case of a total propagation time of 12.1 ps (5×10^5 a.u., to be comparable with the previous calculations), and with the choice $E_0 = 5.58 \times 10^5$ V/cm. (No adjustment of E_0 to prevent large intensities has been made in the case of larger aggregates.) In the case of the dimer, after 12.1 ps the switching is complete. For larger systems, the yield of the all-cis form is still incomplete after 12.1 ps, but continues to steadily increase with time. Therefore, a longer irradiation time will eventually lead to high yields.

In passing, we note that the same strategy works also for systems with four-level monomers. For the dimer, the excited-state subsystem Hamiltonian gives four transition frequencies. The final target yield after 12.1 ps is about 0.92 and keeps increasing.

IV. CONCLUSION

In conclusion, we have devised simple models for aggregates of molecular monomers which can be electronically excited, are coherently coupled to each other, and are at the same time embedded in a dissipative environment. The goal was to optically transform the "ensemble" from a collective ground state, to another stable state in which all monomers have switched. The initial and target states are not directly connected through any coherent or incoherent coupling. A concrete example is photoswitching of an ordered set of azobenzene molecules on a solid surface, however, we do not claim that the present model is realistic for the understanding, of self-assembled azobenzene monolayers. Since the model is coarse grained, it may also serve other purposes, such as problems related to molecular electronics and energy transport in complex systems. For the sake of generality we took up to N-exciton states into account, which may not always be necessary in practice.

We devised various strategies to achieve the goal of collective switching. A coherent pump-dump scheme realized with short laser pulses or pulse sequences works typically only partially, in particular when the exciton states broaden to bands and the resonance conditions are not easily met. Both $\sin^2$-shaped pulses and pulses computed by an optimal control algorithm work well in the dimer case. For larger aggregates, only the optimal control derived pulses were successful. Various laser distillation schemes were found to be promising. In these, the system is repeatedly pumped coherently, for instance, with a short, broadband pulse. From the intermediate state(s), the system relaxes back to the initial and final states. Even if the incoherent population of the target state occurs with low probability during a single shot, it accumulates during the distillation process until the target is achieved. A target yield of almost 100% can be achieved with pulse lengths above 20 fs. With shorter pulses, target yields do not reach 100% due to a spectral overlap.

It will be interesting to extend these ideas to larger aggregates (possibly treated within a mean field approximation), and to achieve other targets, such as patterning, or the entanglement control in molecular arrays.[3]

ACKNOWLEDGMENTS

We acknowledge support by the Deutsche Forschungsgemeinschaft through SFB 658 on *Elementary Processes in Molecular Switches at Surfaces*, project C2.

[1] Zhen Huang and Sabre Kais, Phys. Rev. A **73**, 022339 (2006).
[2] D. DeMille, Phys. Rev. Lett. **88**, 067901 (2002).
[3] Q. Wei, S. Kais, and Y. P. Chen, J. Chem. Phys. **132**, 121104 (2010).
[4] J. Roden, A. Eisfeld, W. Wolff, and W. T. Strunz, Phys. Rev. Lett. **103**, 058301 (2009).
[5] H. van Amerongen, L. Valkunas, and R. van Grondelle, *Photosynthetic Excitons* (World Scientific, Singapore, 2000).
[6] M. Kasha, Radiat. Res. **20**, 55 (1963).
[7] C. Gahl, R. Schmidt, D. Brete, E. R. McNellis, W. Freyer, R. Carley, K. Reuter, and M. Weinelt, J. Am. Chem. Soc. **132**, 1831 (2010).
[8] Z. Wang, A.-M. Nygard, M. J. Cook, and D. A. Russell, Langmuir **20**, 5850 (2004).
[9] S. Beyvers, Y. Ohtsuki, and P. Saalfrank, J. Chem. Phys. **124**, 234706 (2006).
[10] J.-Å. Anderson, R. Petterson, and L. Tegnér, J. Photochem. **20**, 17 (1982).
[11] H. Fliegl, A. Köhn, C. Hättig, and R. Ahlrichs, J. Am. Chem. Soc. **125**, 9821 (2003).
[12] G. Füchsel, T. Klamroth, J. Dokić, and P. Saalfrank, J. Phys. Chem. B **110**, 16337 (2006).
[13] A. Toniolo, C. Ciminelli, M. Persico, and T. J. Martínez, J. Chem. Phys. **123**, 234308 (2005).
[14] T. Nägele, R. Hoche, W. Zinth, and J. Wachtveitl, Chem. Phys. Lett. **272**, 489 (1997).
[15] A. Bartana, R. Kosloff, and D. J. Tannor, J. Chem. Phys. **99**, 196 (1993).
[16] Y. Ohtsuki, W. Zhu, and H. Rabitz, J. Chem. Phys. **110**, 9825 (1999).
[17] A penalty factor $\alpha = 0.1$ a.u. was used [see Eq. 12 of Ref. 9]. The control fields were further forced, by narrow $\sin^2$ functions, to go smoothly to zero at the boundaries of the control interval.
[18] G. K. Paramonov and P. Saalfrank, Chem. Phys. Lett. **301**, 509 (1999).
[19] M. Shapiro, E. Frishman, and P. Brumer, Phys. Rev. Lett. **84**, 1669 (2000).
[20] E. Frishman, M. Shapiro, and P. Brumer, J. Phys. B: At. Mol. Opt. Phys. **37**, 2811 (2004).
[21] D. Gerbasi, M. Shapiro, and P. Brumer, J. Chem. Phys. **124**, 074315 (2006).
[22] S. S. Bychkov, B. A. Grishanin, and V. N. Zadkov, Laser Phys. **11**, 1088 (2001).
[23] J. C. Tremblay and P. Saalfrank, J. Chem. Phys. **131**, 084716 (2009).
[24] V. M. Marchenko, V. V. Koltashev, S. V. Lavrishchev, D. I. Murin, and V. Plotnichenko, Laser Phys. **11**, 330 (2001).